J. nat. Rubb. Res., **12(4)**, 199–214

Rolling-ball Rubber-layer Isolators[†]

A.H. MUHR[*#], M. SULONG[*] AND A.G. THOMAS[**]

A system has been developed for seismic isolation of light structures, with no restriction as to choice of deflection capacity, damping or period. It comprises: isolators consisting of balls rolling between tracks; damping provided by layers of dissipative material, such as rubber, bonded to the tracks and hence integral with the isolators; separate springs to provide a restoring force.

The use of rubber layers to provide rolling resistance permits a very wide choice of effective damping level, and the rolling resistance can easily be arranged to be a preset function of displacement. The design of the isolators is thus more versatile than for sliding isolators, which are otherwise similar in concept.

Experimental results are presented for the steady rolling resistance as a function of load, ball radius, rubber thickness, rubber nature and rolling velocity. The peak in horizontal force required to start the balls rolling depends on the length of time for which the load is applied before rolling starts as well as on the above parameters. This peak in force could be beneficial in providing resistance to wind loads, but if too high could prevent the isolation system operating in an earthquake.

It is difficult to design economical laminated rubber isolators that support light structures and achieve values of horizontal period and deflection capacity required by seismic isolation systems. These required values are much the same whatever the weight of the isolated structure, with the deflection capacity being controlled mainly by the plan dimension of the bearings[1] while the period T is given by:

$$T = 2\pi \sqrt{\frac{M}{K}} \qquad \dots 1$$

where M is the mass of the isolated structure and K is the combined horizontal stiffness of the bearings. Thus, for a low value of M we must design bearings of low stiffness. This is difficult to reconcile with keeping their width constant[1], since to make the stiffness low we need either to make the bearings very high, with a lot of laminations to maintain stability, or to construct a composite bearing by linking together an array of bearings of reduced width with plates at several intermediate heights, again to control stability[2]. As well as making design difficult, such bearings will be costly to make.

[†] Paper presented at the International Rubber Conference 1997 Malaysia, 6–9 October, Kuala Lumpur

[*] Tun Abdul Razak Research Centre, Brickendonbury, Hertford SG13 8NL, United Kingdom

[**] Materials Department, Queen Mary and Westfield College, University of London, London E1 4NS, United Kingdom

[#] Corresponding author

The problem with using laminated bearings for light structures arises from the combination of the spring and isolator functions. A system has been developed[3] which separates these functions and hence enables isolation of even very light structures, with no restriction as to the choice of deflection capacity, damping or period. It comprises:

- Isolators consisting of balls rolling between tracks
- Damping provided by layers of dissipative material, such as rubber, bonded to the tracks and hence integral with the isolators
- Separate springs to provide a restoring force.

The use of rubber layers to provide rolling resistance permits a very wide choice of effective damping level by choosing layers of different thickness (zero thickness giving zero damping) and compounds with different levels of hysteresis. The rolling resistance can easily be arranged to be a preset function of displacement by varying the thickness and/or the rubber formulation (and hence hysteresis) with distance along the rolling path. The design of the isolators is thus more versatile than for sliding isolators, which are otherwise similar in concept.

The basic force-displacement characteristic of the rolling-ball isolation system is shown in *Figure 1*. The slope of the hysteresis loop gives the stiffness K which determines the period T of the system (*Equation 1*) while the area of the loop, proportional to the rolling resistance F_R, controls the damping coefficient of the system.

This paper is concerned only with the rolling resistance, and how it is influenced by the choice of rubber, its thickness, the load on the ball and the radius of the ball.

THEORY

Relationship of Rolling Friction to Indentation Work and Hysteresis

We define the frictional force Q as the work done when the ball rolls a unit distance on a single viscoelastic track. *Figure 2* shows possible schemes for measuring Q. According to Gent and Henry[4], the work of indentation U is in effect applied and relaxed $1/2a$ times in unit rolling distance, where a is the contact radius; thus, if we assume a fraction α of the indentation is lost on each cycle we have:

$$Q \simeq \alpha\, U/2a \qquad \ldots 2$$

The friction ratio μ is given by:

$$\mu = Q/W \simeq \alpha\, U/2aW \qquad \ldots 3$$

Theoretical Equation for Rolling Friction for an Infinitely Thick Layer

According to Hertz the contact radius a and indentation depth d for an elastic half space of Young's modulus E are given by[5]:

$$a = \left[\frac{3}{4}\, WR \left(\frac{1-\nu^2}{E}\right)\right]^{\frac{1}{3}} = \left[\frac{9}{16}\,\frac{WR}{E}\right]^{\frac{1}{3}} \qquad \ldots 4$$

$$d = a^2R = \left(\frac{9}{16}\right)^{\frac{2}{3}} \left(\frac{W}{E^2R}\right)^{\frac{1}{3}} \qquad \ldots 5$$

where Poisson's ratio υ has been set to the value for rubber, 0.5. The indentation work may be calculated from *Equation 5*:

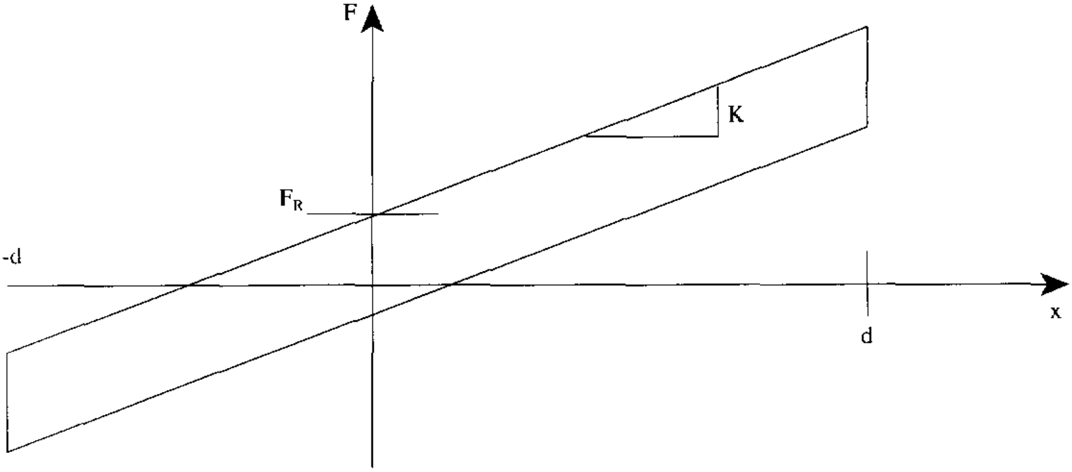

Figure 1 Schematic hysteresis loop for isolation system consisting of rolling-ball isolators and springs

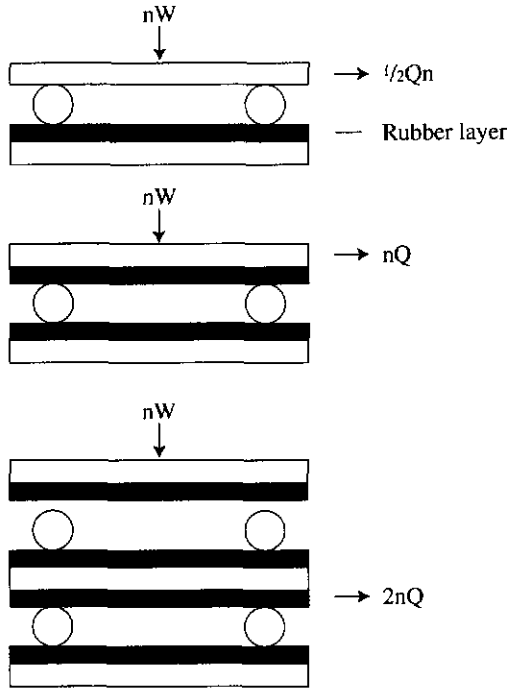

Figure 2 Possible arrangements of balls and rubber layers for isolators or for experimental determination of rolling resistance, n *is the number of balls in one layer*

$$U = \int_0^d W dx = \frac{16}{9} ER^{\frac{1}{2}} \int_0^d x^{\frac{3}{2}} dx$$

$$= \frac{2}{5} \cdot \frac{16}{9} ER^{\frac{1}{2}} d^{\frac{5}{2}}$$

$$= \frac{2}{5} \left(\frac{9}{16}\right)^{\frac{2}{3}} \left(\frac{W^5}{E^2} R\right)^{\frac{1}{3}} \qquad \ldots 6$$

Combining *Equations 3, 4* and *6* we find:

$$\mu_\infty \cong \frac{1}{5} \left(\frac{9}{16}\right)^{\frac{1}{3}} \left(\frac{W}{ER^2}\right)^{\frac{1}{3}} \alpha$$

$$\simeq 0.165 \left(\frac{W}{ER^2}\right)^{\frac{1}{3}} \alpha \qquad \ldots 7$$

where the subscript ∞ refers to an infinitely thick layer. *Equation 7* has been proposed in several publications albeit with different values for the numerical coefficient, as reviewed by Gent and Henry[4].

Theoretical Equation for a Layer of Finite Thickness

Waters[6] carried out an experimental investigation of the effect of rubber layer thickness on the indentation. His experiments covered the regime of small loads and indentations for which it may be reasonable to assume that a and d are related to each other in the same way as in the Hertz theory (see *Equation 5*):

$$a \simeq \sqrt{dR} \qquad \ldots 8$$

and d is modified from the Hertzian value d_∞ at $t = \infty$ (given by *Equation 5*) according to:

$$d = d_\infty f(t/a) \qquad \ldots 9a$$

where the function $f\ (t/a)$ was determined empirically as:

$$f(t/a) \simeq 1 - \exp(-At/a) \qquad \ldots 9b$$

where A has the values 0.417 and 0.67, respectively for bonded and lubricated boundary conditions at the back of the rubber sheet.

To calculate the indentation work we need to express W in terms of d. Substituting *Equation 5* for d_∞ as a function of W, and *Equation 8* for a as a function of d, into *Equation 9* we find:

$$W = \left(\frac{d}{f(t/\sqrt{Rd})}\right)^{\frac{3}{2}} ER^{\frac{1}{2}} \frac{16}{9}$$

$$= (E t^3/R)(16/9)g(s) \qquad \ldots 10$$

where $g(s) = [(s^2/f(s^{-1})]^{\frac{3}{2}}$ and $s = \sqrt{(Rd)}/t$. Rearrangement of *Equation 10* would enable E to be calculated from s (and hence d). Inversion of the equation shows that s is a function of the non-dimensional group (WR/Et^3).

Thus $\quad U = \int_0^d W dx$

$$= (E t^3/R)(16/9)\ (2t^2/R) \int_0^s g(s).sds$$

If we write the integral as I(S) we see that:

$$U = (Et^5/R^2)\ (32/9)\ \mathrm{I(S)} \qquad \ldots 11a$$

From *Equation 9* we see that $1/f(s^{-1})$ is unity at $s = 0$ and rises monotonically as s increases. It may be deduced that:

$$S^5/5 < \mathrm{I(S)} < (S^5/5)[f(S^{-1})]^{-3/2} \qquad \ldots 11b$$

If we substitute *Equation 11a* into *Equation 3* and express a in terms of d using *Equation 8* we find an expression for μ as a function of d:

$$\mu = \frac{\alpha}{2W} d^{-1/2} R^{-1/2} (Et^5/R^2)(32/9)\,\mathrm{I(S)}$$
$$= \alpha\,(16/9)(Et^4/R^2W)\,S^{-1}\,\mathrm{I(S)}$$
$$= \alpha\,(16/9)\,(W/R^2E)^{1/3}\,(Et^3/WR)^{4/3}\,S^{-1}\,\mathrm{I(S)}.$$

Using *Equation 7* to express $\alpha(W/ER^2)^{1/3}$ in terms of the rolling friction ratio μ_∞ for a semi-infinite layer and *Equation 10* to express (Et^3/WR) in terms of S we find finally that:

$$\mu = \mu_\infty \cdot 5[f(S^{-1})]^2\,S^{-5}\,\mathrm{I(S)} \equiv \mu_\infty \Phi(S) \quad \text{... 12a}$$

The non-dimensional quantity Φ, a function of RW/Et^3, should tend to unity as $W \to 0$ or $t \to \infty$ and to zero as $t \to 0$. From inequality (*Equation 11b*) we may further deduce that:

$$[f(S^{-1})]^2 < \Phi < [f(S^{-1})]^{1/2} \quad \text{... 12b}$$

The predictions of the theory are presented in the dimensionless plot of *Figure 3*. The ordinate μ/μ_∞, is equal to Φ(S) from *Equation 12*, and is calculated using *Equations 9, 11* and *12* by numerical integration, making use of the bounds (*Equation 11a* and *Equation 12a*) to make sure the results are sensible when s is small. The abscissa $(t/R)/(W/ER^2)$, is equal to $[(16/9)\,\mathrm{g(S)}]^{-1/3}$ from *Equation 10* and is calculated using *Equation 9*. To construct the plot, the parameter s is varied over a sufficiently wide range.

From *Figure 3* the theory predicts that the Hertzian theory is applicable when

$$(t/R) \geq 10(W/ER^2) \quad \text{... 13}$$

Scaling Rules and Dimensional Analysis

It is desirable to identify scaling rules, so that experiments carried out on one scale may be used to predict the value of μ at other scales. If linear dimensions are scaled by λ, we have:

Ball radius $R \to \lambda R$
Rubber thickness $t \to \lambda t$ ... 14a

It follows that to keep the stresses the same (and hence all dimensionless quantities such as strains and angles) the load W must be scaled by λ^2:

Load $W \to \lambda^2 W$ ... 14b

Being dimensionless, the friction ratio μ should be unaltered if W is scaled as in *Equation 14b*. Because the hysteretic factor α may depend on rate the rolling velocity v should, strictly, also be scaled so as to keep the frequency $v/2a$ constant:

Velocity $v \to \lambda v$ ... 14c

It follows from *Equation 14a* and *Equation 14b* that for one rubber at one rate μ must depend only on W/R^2 and t/R. If, futhermore, the rubber properties enter only through the parameters E and α, it should be possible to construct master plots of μ/α *versus* t/R with W/ER^2 as the parameter. Examples of such plots, based on the theory given above for layers of finite thickness and low loads, are given in *Figure 4*. This figure is derived from *Figure 3* by multiplying both the ordinate and the abscissa values by $(W/ER^2)^{1/3}$. Based on the literature, reviewed by Gent and Henry[4], we would expect the theory to be satisfactory provided W/E^2R is sufficiently low. Although the shape of the graphs at high normalised stress

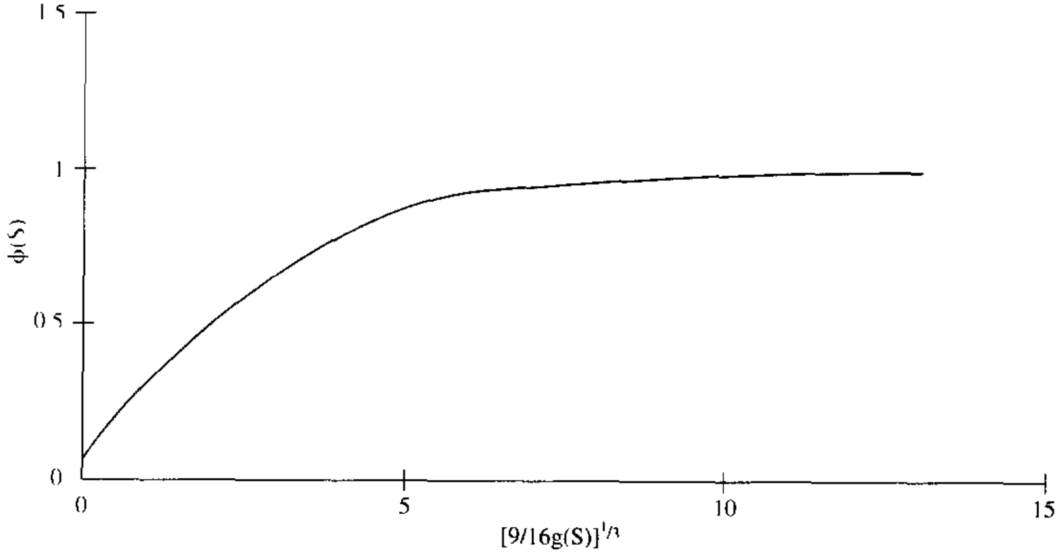

Figure 3 Theoretical plot of reduced friction ratio versus *reduced rubber thickness* (Equation 12)

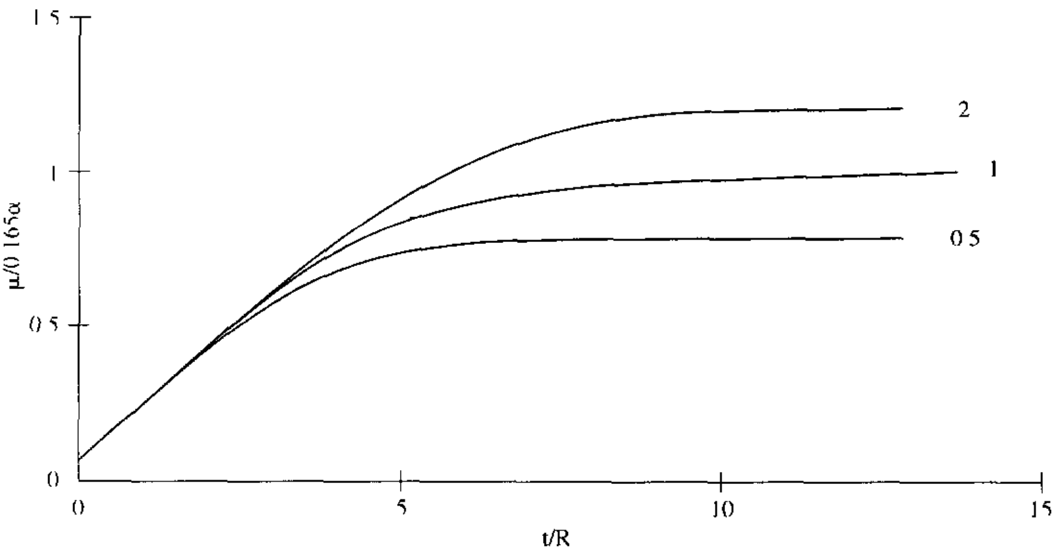

Figure 4 Theoretical plots of friction ratio μ*, scaled using hysteresis parameter* α*,* versus *ratio of rubber layer thickness* t *to ball radius* R *[Equations (12) and (7)] Parameter is* W/ER^2

may not collapse onto the single plot of *Figure 3*, it should be possible to present them in the manner of *Figure 4*, albeit with shapes diverging from the theoretical plots when W/ER^2 is large

EXPERIMENTS

Materials and Testpieces

The formulations, standard physical properties and dynamic shear properties of the rubbers used are given in *Table 1*.

The rubber was bonded to steel rolling plates (74×145×12 mm) in layers of various thicknesses. The rubber surfaces were moulded against *Mylar* (polyester film) to produce a good, smooth, surface profile and to keep it clean. Bonding was achieved during vulcanisation using *Chemlok 220*, either directly to the rolling plates or (for earlier testpieces) to 0.1 mm thick aluminium foil which was subsequently stuck to the rolling plates using double-sided adhesive tape.

Unless otherwise stated the surface of the rubber layers, on which the balls were rolled, were dusted with talc.

Method and Procedure

The experimental arrangement is shown in *Figure 5*. In all cases, a set of four balls was used between the rolling plates, the crosshead speed was 1 mm min^{-1} and the temperature was 23±2°C. The rolling unit was connected to the load cell and crosshead of the Instron machine by nylon-coated multistrand wire. The coated wire was hooked to the top rolling plate, passed through the pulley and fixed securely by the pin of the load cell. The apparent stiffness of the pulling cable, measured using the same load cell and crosshead arrangement, was 13 Nmm^{-1} Also the horizontal and vertical alignments of the wire were adjusted visually so that they always remained parallel to the centre of the balls (*i.e* rolling unit) and crosshead (load cell) of the machine, respectively, when the top plate with the mass moved forward. The load cell and cross head position outputs were connected to an XY recorder.

When the crosshead of the Instron machine travels upwards, it pulls the cable. Since the cable was hooked to the rolling unit the tension rises until the top rolling plate starts to move forward. This leads to a peak in the force as shown in *Figure 6*. The tension then falls to a minimum, perhaps enhanced by the tendency of the mass (once accelerated) to travel under its momentum. This occurs for a very short time, before a steady rolling speed is achieved (*i.e* steady state rolling frictional force). One disadvantage of this technique is the difficulty of obtaining a straight rolling path particularly for low rolling friction conditions such as for a low normal load, with highly resilient talced rubber.

In order to check the reliability of the technique, a separate experiment was carried out using steel balls (3.175 mm radius) but no rubber layer. All other parameters remained the same except the normal load was applied starting from zero and the balls were rolled either directly on the steel plate or on the aluminium sheet alone which was held to the rolling plate by double-sided adhesive tape. When the Instron crosshead was run at 1 mms^{-1} with no mechanical connection between load cell and the roller assembly, the electrical noise in the load cell output, as measured on the xy

TABLE 1 FORMULATIONS OF THE RUBBER COMPOUND USED IN THE EXPERIMENT

Ingredients	No. 1 (p.p.h.r.)	No. 3 (p.p.h.r.)	No. 4 (p.p.h r.)
Natural rubber (SMR CV60)	100	100	
NBR (*Breon N41C80*)			100
Zinc oxide	5	5	5
Stearic acid	2	2	2
Santoflex 13	3	3	1
Antilux 600	3	3	–
Curatives:			
Sulphur	1	0.6	2.5
CBS	0.75	0.45	0.5
Cure time (min)	50	50	45
Cure temp. (°C)	140	140	150
Hardness (IRHD)	34	28	51
Tensile properties:			
M100 (MPa)	0.60	0.42	1.19
TS (MPa)	15.1	6.70	14.7
EB (%)	702	974	565
Lupke rebound resilience (%)	80.1	73.9	19.7
Dynamic properties 50% strain, 0.01 Hz:			
G (MPa)	0.32	0 24	0.72
δ (°)	1.3	3 0	5.3
50% strain, 0.1 Hz:			
G (MPa)	0 33	0.26	0.81
δ (°)	1.4	3.8	6.7
50% strain, 1 Hz.			
G (MPa)	1.34	0 28	0 94
δ (°)	2.2	4.9	7 9

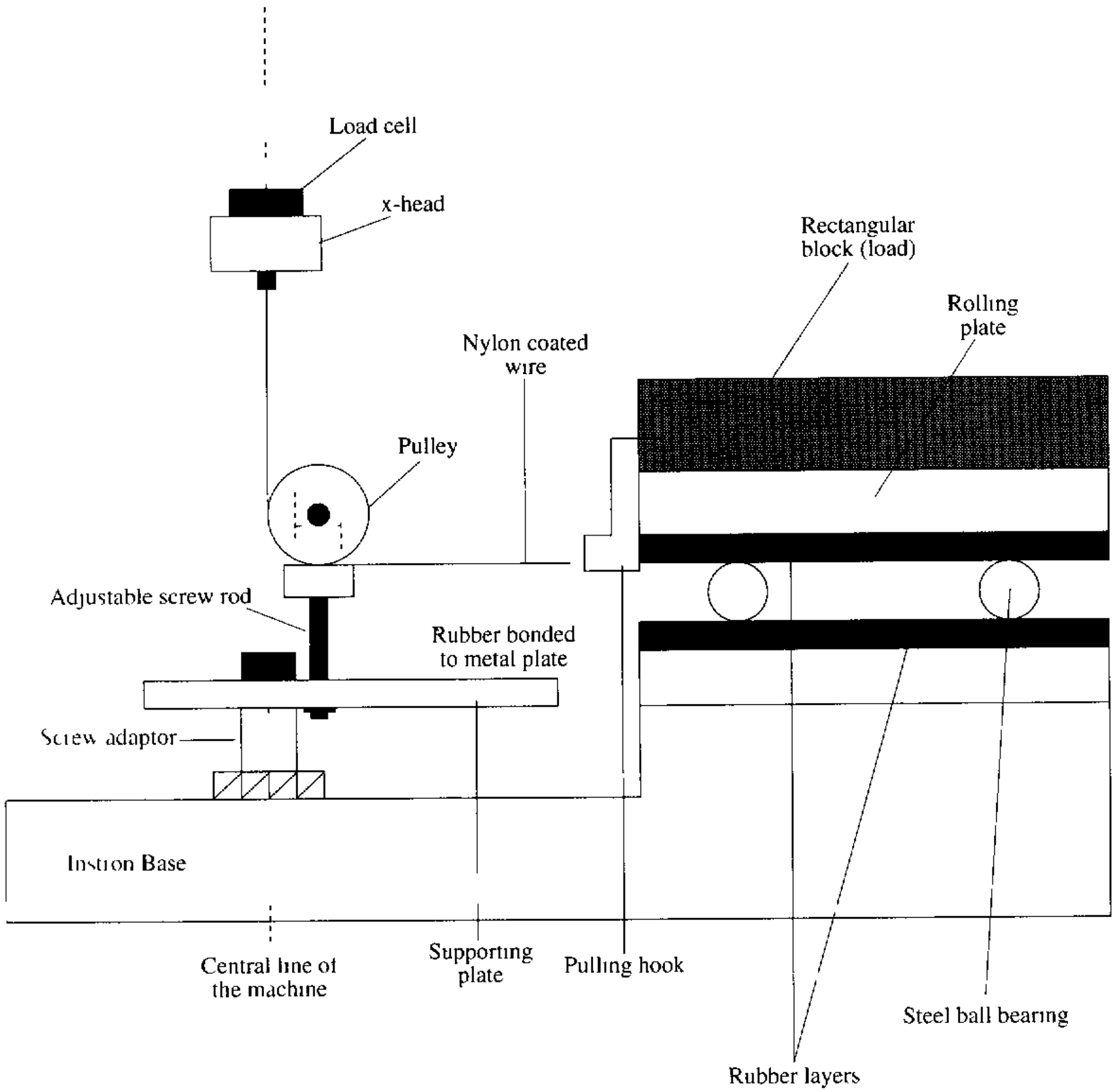

Figure 5 Apparatus for measuring rolling forces

chart recorder, corresponded to 0.0015 N (peak to peak). In the case of rolling directly on the steel, the plate does not roll smoothly or in line with the pulling direction because of the machining marks on its surface. The peaks in horizontal force are about 0.2 N for a total normal load of 10 N. If the steel plates were replaced with glass plates it was not possible to level sufficiently accurately to prevent spontaneous rolling, while peak forces of only about 0.03 N for a load of 46 N were recorded. It was found that with aluminium sheet bonded to the steel the results were consistent with a steady rolling friction coefficient of about 0.06 and a peak roll-out value about 30% higher for total normal loads in the range 10 N–72 N. Because this value is rather high, the use of the aluminium backing foil (and double-sided tape) was abandoned for later experiments; instead the rubber layers were bonded directly to the steel backing plates using *Chemlok 220.*

RESULTS

Effect of Load and Rubber Thickness

A lightly crosslinked unfilled NR compound was used for these tests (No.3, *Table 1*). Layers of this rubber were bonded directly to rigid steel plates during vulcanisation. Nine thicknesses, ranging from 0.254 mm to 3.70 mm, were used. Balls of the following radii were used: 1.58, 2.0, 2.5, 3.0, 3.175, 3.5, 3.76, 4.0, 5.0, 6.0 and 6.25 mm. When the ball size was changed the load W per ball was also changed in such a way that the stress parameter W/R^2 was held constant over the range of t/R values investigated. Three levels of applied stress were used, corresponding to $W/R^2 = 1.0$, 2.0 and 5.2 MPa.

The steady-state rolling resistance results for $W/R^2 = 1$ MPa are given in *Figure 7*. The results collapse onto a single curve, regardless of scale. This shows that the scaling rule works, despite the cross-head speed being kept constant at 1 mms^{-1}. Presumably the effect of rate is very weak. *Figure 8* includes results for the higher values of W/R^2 as well. The steady state rolling frictional coefficient rises as the thickness of the rubber layer is increased and tends to plateau.

A comparison was made between the plateau value of μ and the theory for a semi-infinite layer (*Equation 7*). The hysteresis parameter was calculated as $\alpha = \pi \sin\delta = 0.208$ from dynamic test results at 0.1 Hz and 50% strain (*Table 1*). The plot of $\mu_{plateau}$ against $0.165 (W/ER^2)^{1/3} \alpha$ is shown in *Figure 9*. At the lower loads there is fair agreement with the theory, although the dependence on load seems to be stronger than predicted so that at the highest load $\mu_{plateau}$ is 35% higher than predicted. The results also conflict with the extension of the theory to rubber layers of finite thickness, since the plateau region seems to be reached at quite low values of t/R, and the results are strongly dependent on the value of W/R^2 even before the plateaux are reached (cf. *Figure 4*).

These departures from the theory may well be a consequence of the high values of W/ER^2 being used, making predictions based on infinitesimal strain theory invalid. Indeed, for the largest of the stresses used (W/R^2 = 5.2 MPa) a permanent rolling track remained on the surface when t/R<0.55. The rolling track is deep, almost reaching the backing plate in the case of the thinner rubber layers so that the blackness of the *Chemlok 220* layer could be seen through the very thin layer of rubber remaining. Obviously, the strains associated with such permanent tracks must be very large.

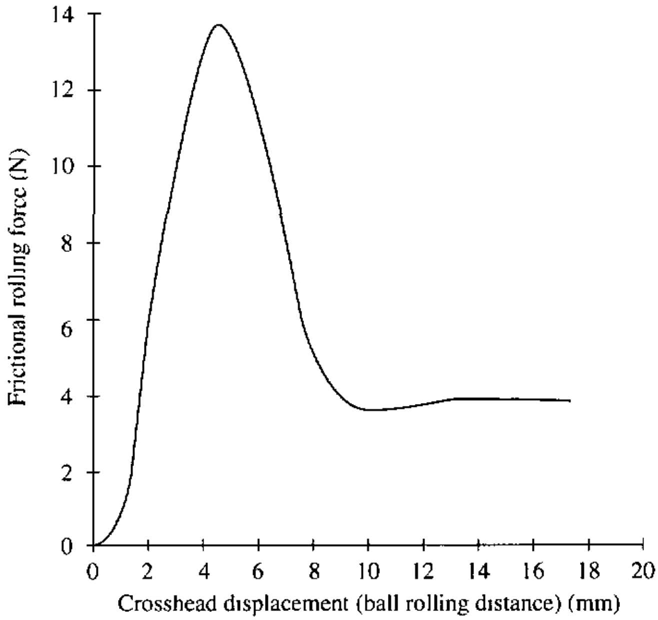

Figure 6. Example of rolling force versus crosshead displacement (NBR Compound No 4, t = 2mm, R = 3.175 mm, total load on the four balls = 90 N, dwell time 1000 min).

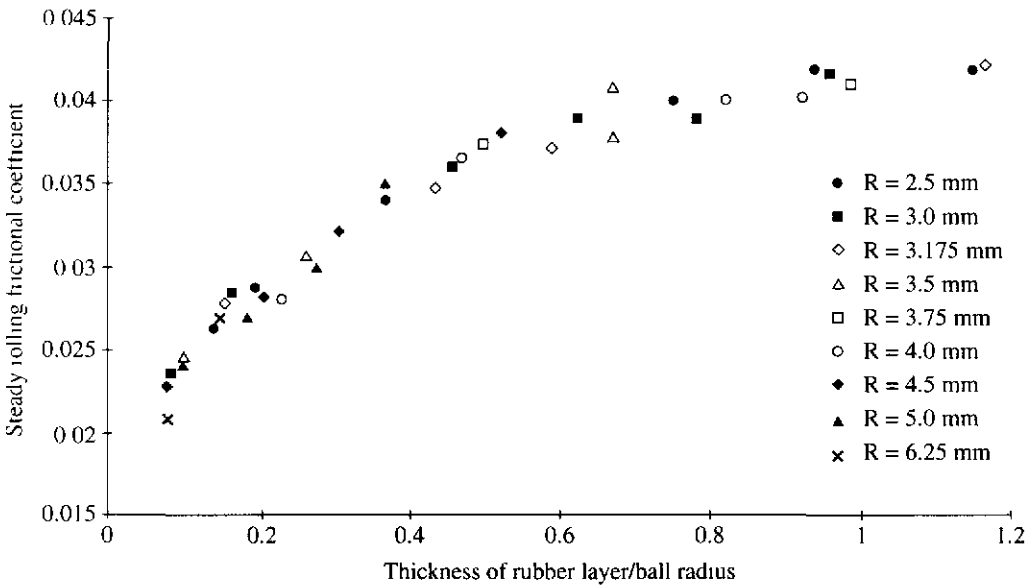

Figure 7. Experimental results for steady rolling friction coefficient on Compound 3 *(for* W/R^2 *held constant at 1.0 MPa) versus ratio of rubber layer thickness* t *to ball radius* R.

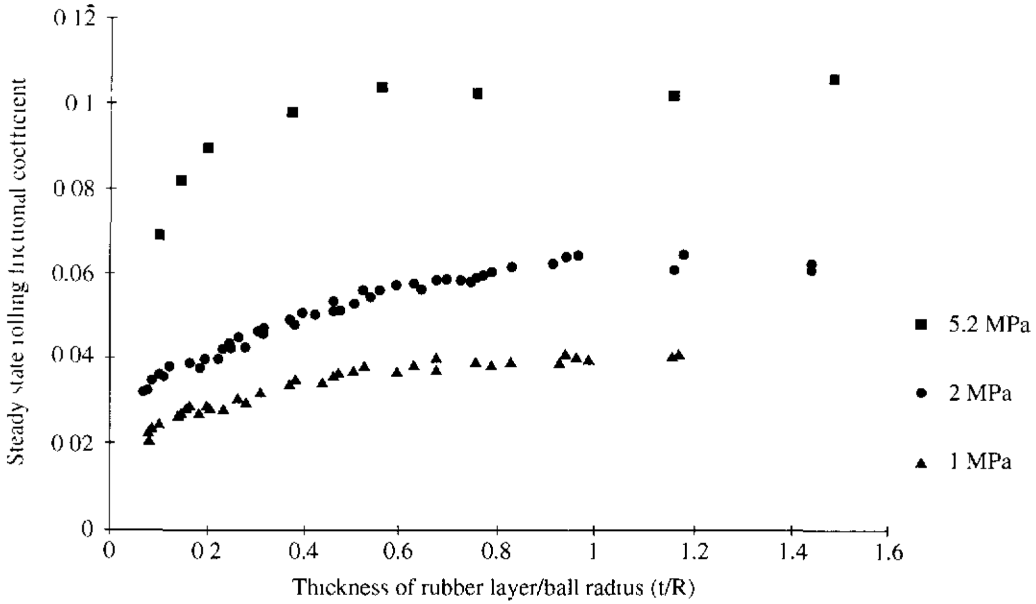

Figure 8 As Figure 7 *but including results at different values of* W/R^2 *(given in MPa as a label for each plot)*

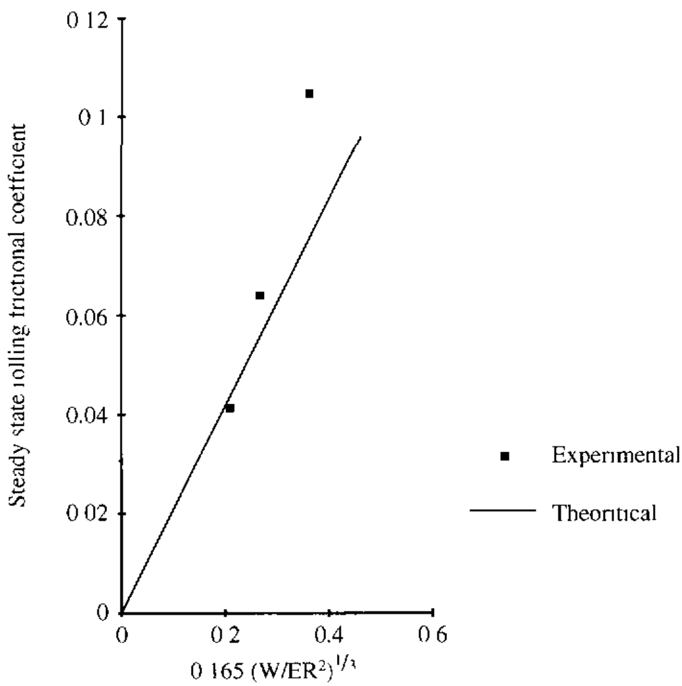

Figure 9. Comparison of theory (Equation 7) *with experimental results of steady state rolling resistance as a function of load.*

No fracture was observed in the rubber and there was no sign of recovery after 4 months. For the lower stresses (W/R^2 = 1 or 2 MPa) the rolling tracks appeared on the rubber surface only temporarily.

Effect of Dwell-time

The peak in the force as the balls roll out from their 'pits' is potentially a problem for the isolation system. If it increases with time it may reach such a high value that the seismic excitation is insufficient to get the system past this peak force, so that it will not operate as intended.

With this in mind a vertical load of 90 N was applied for designated periods of time to sets of four balls (R = 3.175 mm, so that W/R^2 = 2.23 MPa) between 2.00 mm thick rubber layers. Three different rubbers were used (see *Table 1*). For NBR the surface was used either clean (*i.e.* immediately after peel of the *Mylar* against which it was moulded) or after dusting lightly with talc. The two NR compounds (see *Table 1*) were investigated only after lightly dusting with talc.

The results for peak roll-out force are given in *Figure 10*. It is apparent that the peak roll-out force increases approximately linearly with the logarithm of time. The rate of increase is greatest for the lightly crosslinked NR *Compound No. 3*. For NBR, the effect of talcing the surface is evidently to reduce the rate of increase in peak roll-out force.

It was found that the steady rolling force does not change within experimental error, for the four different rubber samples, over the period of 9 months. *Table 2* gives the average values. The steady rolling force was reduced by approximately 13% when the NBR was talced.

TABLE 2. MEAN STEADY ROLLING FRICTION RESULTS FOR PEAK ROLL-OUT FORCE EXPERIMENTS REPORTED IN *FIGURE 10*
(W/R^2 = 2.23 MPa, t/R = 0.63)

Rubber	μ
No. 4 (NBR) clean	0.048
No.4 (NBR) talced	0.040
No. 1 (NR) talced	0.017
No. 3 (NR) talced	0.037

The ratio of peak roll-out force to the steady rolling force is highest for the rubbers with higher damping.

The indentation marks or 'pits' on the rubber surfaces are sharply defined after 9 months dwell time, but gradually recovered with time after unloading, being still visible after two months. One way of assessing the recovery is to locate the balls back in the pits at designated times and immediately measure the peak roll-out force. This force falls as recovery proceeds. Such experiments confirmed that recovery is only partial after two months (see *Table 3*). It also shows that the physical formation of 'pits', presumably due to creep, is the main cause of the rise in peak roll-out force with time, at least for talced samples.

DISCUSSION AND CONCLUSIONS

The results confirm that useful magnitudes of rolling resistance can be achieved with the rolling-ball dissipative-layer geometry, using fairly standard rubber compounds. Calculations of the damping ratio of a linear system

TABLE 3 EVALUATION OF PIT RECOVERY AFTER 9 MONTHS DWELL TIME OF NBR (*COMPOUND NO 4*) AND NR (*COMPOUND NO 1* AND *3*). [NORMAL LOAD PER BALL = 22 5 ± 0.2 N, R = 3 175 MM]

	NBR *Compound No 4* (t = 0.5 mm)	(t = 2.0 mm)	NR *Compound No. 1* (t = 2.0 mm)	NR *Compound No 3* (t = 2 mm)
1–2 minutes dwell time under constant normal load:				
F_0 = Roll-out frictional force per ball (N)	1.28	1.74	0.76	1.45
9 months dwell time under constant normal load:				
F = Roll-out frictional force per ball (N)	2.42	5.65	2.45	6.35
2 minutes pit recovery from 9 months dwell time:				
F_{r1} = Roll-out friction force per ball (N)	2.41	5.21	2.38	4.5
% Recovery = $\frac{F - F_{r1}}{F - F_0}$	1	12	4	38
2 months pit recovery from 9 months dwell time:				
F_{r2} = Roll-out frictional force per ball (N)	2 29	4.00	1.61	2 58
% Recovery = $\frac{F - F_{r2}}{F - F_0}$	12	42	50	77

equivalent to *Figure 1* show that it should be relatively easy to achieve values in the typical design range of 0.1 to 0.3, for typical design values of the period *T*.

Although the system behaves well for the largest stresses used (W/R^2 = 5.2 MPa), the generation of deep semi-permanent rolling tracks at this stress level suggests it should be an upper bound for design purposes. As this loading is relatively modest, from the point of view of designing an economical system, it is clear that for all but the lightest structures it is desirable to use a design level for W/R^2 of at least 1 MPa. This stress is still quite large in the context of indentation in rubber; *Figure 9* and a comparison of *Figures 4* and *8* suggest it is beyond the regime of validity of Hertzian

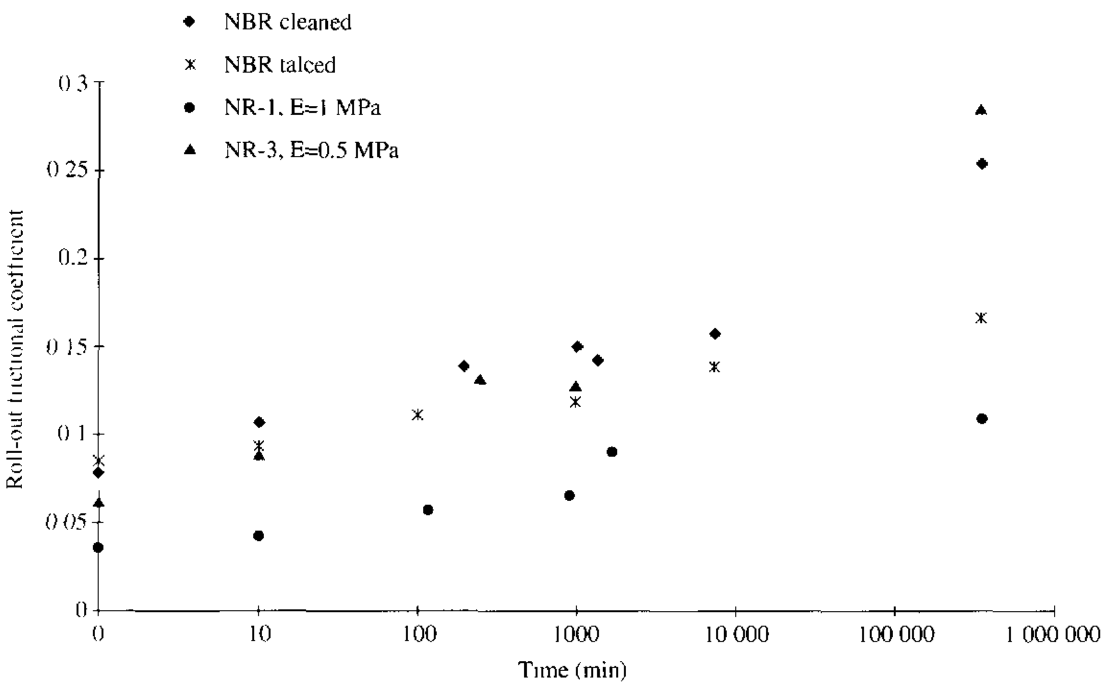

Figure 10 Effect of dwell time on roll-out friction coefficient.

indentation theory or of Waters' empirical modification for layers of finite thickness. In the absence of a method of predicting the rolling resistance theoretically, reliance will have to be placed on prototype test results. However, the experiments are quite straightforward and it is relatively easy to change the rubber compound or its thickness to achieve a target rolling resistance.

The mechanism of generation of the frictional resistance is confirmed to be the hysteresis losses from the moving indentation, as reviewed by Gent and Henry[4], since there is a strong correlation with the loss tangent of the rubber while the state of the rubber surface (clean or talced) has a relatively weak effect.

If the balls are held stationary under load for a prolonged dwell-time the peak in force, occurring just before the onset of steady rolling, rises approximately linearly with log time. In the worst case, corresponding to the lightly crosslinked NR *Compound No. 3* after 9 months dwell time, the peak force is 7.6 times the steady rolling value. Such high peak values are a potential problem for the system, since it would not operate correctly unless the seismic excitation is large enough to roll the balls out of their 'pits'. The problem would be serious if the peak roll-out force exceeds the maximum shear force capability of the isolated structure. One method of mitigating this potential problem is to site the balls on regions of very thin (or more resilient) rubber under static conditions, so that a high roll-out force does not develop. Once rolling, though, the balls could roll onto regions of thicker or more hysteretic rubber to achieve the design level of rolling resistance.

It is concluded that the prolonged isolation system has the necessary versatility to meet typical design requirements. The lighter the structure, the more economic should the system be, since fewer balls will be required. In this way it complements systems based on laminated rubber bearings, since these become relatively more complicated and costly the lighter the structure.

REFERENCES

1. GREGORY, I.H. AND MUHR, A.H. (1995) Design of Elastomeric Antiseismic Bearings. *European Seismic Design Practice: Research and Practice. Proc. 5th SECED Conference, (Elnashai, A.S. ed.)*. Rotterdam: Balkema.

2. DERHAM, C.J. AND THOMAS, A.G. (1980) The Design and Use of Rubber Bearings for Vibration Isolation and Seismic Protection of Structures. *Eng. Struct* **2**, 171.

3. COOK, J.W., MUHR, A.H., SULONG, M. AND THOMAS, A.G. (1997) Rolling Ball Isolation System for Light Structures. *Proc. post SMiRT Conference Seminar on Seismic Isolation, Passive Dissipation and Active Control of Seismic Vibrations of Structures, Taormina, Italy, August 1997.*

4. GENT, A.N. AND HENRY, R.L. (1969) Rolling Friction on Viscoelastic Substrates. *Trans. Soc Rheol.*, **13**, 255.

5. TIMOSHENKO, S. (1934) *Theory of Elasticity*. New York: McGraw Hill.

6. WATERS, N.E. (1965) The Indentation of Thin Rubber Sheets by Spherical Indentors. *Brit J. Appl. Phys.*, **16**, 557.